JOURNAL OF MATERIALS SCIENCE 31 (1996) 5829–5834

Fabrication and microstructure of ZrO_2–Ni functional gradient material by powder metallurgy

J. C. ZHU, Z. D. YIN, Z. H. LAI
Department of Metals and Technology, Harbin Institute of Technology, Campus Box 433, Harbin 150001, People's Republic China

Functional gradient material (FGM) of the ZrO_2–Ni system was developed by a powder metallurgical process, and investigated for its microstructure by means of X-ray diffractometry (XRD), electron probe microanalysis (EPMA), transmission electron microscopy (TEM) and optical microscopy. It was shown that the sintered body of ZrO_2–Ni FGM is almost fully densified, and its chemical composition and microstructure have the expected gradient distribution. With composition variation, the microstructure changes gradually from zirconia particles dispersed in a nickel matrix to the converse with nickel particles dispersed in a zirconia matrix, with network structures in the intermediate composition range. Therefore, no distinct interfaces appear in the FGM due to the gradient change of components, that is, both zirconia and nickel are present everywhere in the microstructure. In phase composition, the sintered ZrO_2–Ni FGM consists of nickel, tetragonal zirconia and a little monoclinic zirconia. No reaction between nickel and zirconia has been detected. The substructure of nickel and monoclinic zirconia are twins, and strain fringes can also be found in zirconia.

1. Introduction

Functional gradient materials (FGM) are multi-component composites with continuous inhomogeneity of composition or structure. The gradient changes of composition and microstructure can reduce or eliminate specific interfaces between constituent materials such as ceramics and metals. Therefore, FGMs display optimal advanced properties or functions, particularly the effective relaxation of thermal stress induced by high temperature variations in service. Since the concept of FGM was first proposed by some Japanese scientists several years ago [1, 2], it has attracted worldwide attention for system components used in the super high-temperature range [3, 4], for example, spaceplanes, gas turbines and fusion reactors. Moreover, FGM can also be applied to the electronics, chemical and biomedical fields as well as many others [5, 6].

Since material properties, such as thermal, electrical and mechanical properties, are strongly dependent on microstructure, it is extremely important to control the microstructural transition to improve and optimize an FGM's performance. Various techniques have been employed in the fabrication of FGMs [7], including physical and chemical vapour deposition, sintering, plasma spraying, galvanoforming and combustion synthesis. Powder metallurgical (P/M) process is one of the most viable routes for FGMs [8], for the composition and microstructure as well as shape forming of FGM can be easily controlled in a wide range. We have developed ZrO_2–Ni FGM by P/M method, and some experimental results on microstructure and mechanical properties have been preliminarily reported [9]. The aim of the present paper is to investigate the P/M fabrication and the microstructural characteristics of ZrO_2–Ni FGM.

2. Experimental procedure

2.1. Fabrication of ZrO_2–Ni FGM

Powders of partially stabilized zirconia (PSZ, doped with 3 mol % yttria) and nickel were chosen as the raw materials (Table I). The powder metallurgical process of the FGM is illustrated in Fig. 1. The raw powders with different PSZ/Ni ratios were first mixed by ball milling for 24 h with ethanol as a solvent. After being dried, the mixed powders were filled in a stepwise sequence according to the pre-designed compositional profile and compacted in a steel die at 150–200 MPa. Then the green compact was hot pressed at 1300–1400 °C under a pressure of 25 MPa for 1–2 h in a nitrogen atmosphere. The subsequent rate of cooling and unloading must be suitably controlled to prevent the sintered body from warping and cracking. In this manner, the FGM as well as uniform composites (non-FGM) with various mixing ratios were obtained. The size of the sintered specimens was about $60 \times 60 \times 6\ mm^3$. Samples for microstructural inspection were cut with a diamond saw, and their surfaces were ground and polished.

0022–2461

TABLE I Raw powders used in the experiment

Powder	Purity (%)	Particle size (μm)	Apparent density ($g\,cm^{-3}$)	Specific surface area (m^2g^{-1})
PSZ	99.8	< 0.5	1.3	10 ~ 15
Ni	99.6	2.5–4	0.8–1.0	–

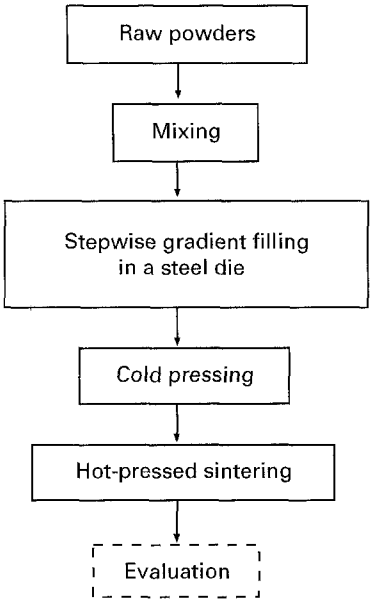

Figure 1 Powder metallurgical process of FGM.

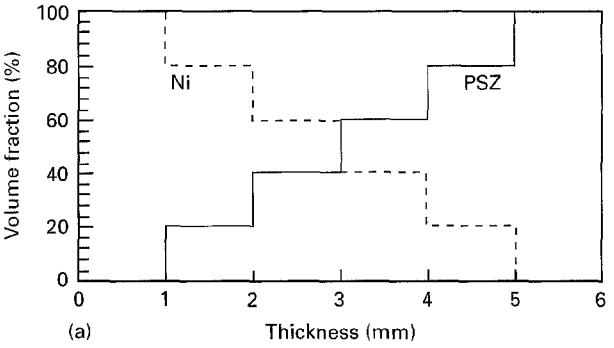

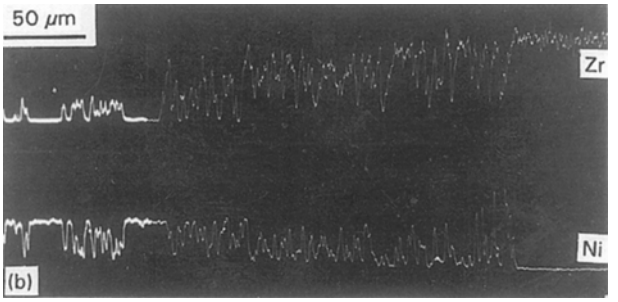

Figure 2 Distribution of chemical composition in ZrO_2–Ni FGM: (a) pre-designed profile and (b) EPMA line analysis of sintered body.

2.2. Observations of microstructure

The density of the sintered samples was measured by Archimedes method. X-ray diffraction (XRD) analysis was conducted to identify the phase structure with D/max-rB X-ray diffractometer, and the amount of monoclinic phase was determined from the relative X-ray diffraction intensities of the two monoclinic peaks $(\bar{1}\,1\,1)$m + (1 1 1)m and the tetragonal peak (1 1 1)t [10]. The microstructure and elemental distribution on the cross-section of the FGM were observed by means of an optical microscope and Jeol JCXA-733 electron probe microanalyser (EPMA), respectively. Samples for EPMA were covered with a thin film of carbon by vacuum deposition. Substructure of the FGM was explored by transmission electron microscopy (TEM) using a Philips CM-12 STEM with 120 kV as the operating voltage. TEM samples were mechanically milled to 0.05 mm thickness with boron carbide abrasive, followed by ion thinning to transparency.

3. Results and discussion

3.1. Distribution of chemical composition

Fig. 2 shows the distribution of chemical composition in cross-section of ZrO_2–Ni FGM. The pre-designed compositional profile is a stepwise type (Fig. 2a), in which composition changes from nickel to zirconia through four interlayers with different PSZ/Ni mixture ratios, and each layer has the same compositional increment of 20% PSZ in volume fraction. The EPMA line analysis of sintered FGM exhibits a gradient elemental distribution of nickel and zirconium, and mainly meets the expected design criteria (Fig. 2b).

3.2. Microstructure

In Figs 3 and 4, the cross-sectional microstructure of the area with compositional change and each layer in ZrO_2–Ni FGM are presented, respectively. The white phase is nickel and the dark one is PSZ. It is observed that the microstructure gradually changes from nickel to zirconia with the variation in composition, and distinct boundaries, such as those in PSZ/Ni direct bonding, disappear (Fig. 3a). Even on the pre-stacked section where chemical compositions jumped in a stepwise manner, both the nickel and zirconia components are continuous in the microstructure.

On the other hand, the FGM exhibits a microstructural transition as shown in Figs 3 and 4, which is typically characteristic in powder metallurgically processed FGMs [11]. In the nickel rich region, the FGM has a dispersed microstructure with PSZ particles in the nickel matrix (Fig. 4a). Typical network structures of nickel can be seen in the microstructures for 40 vol % PSZ (Fig. 4b). The microstructure for 60 vol % PSZ takes the form of loosened connectivity of the metal phase and some agglomerates' can also be observed in the microstructure (Fig. 4c). As the PSZ content increases to 80 vol %, the microstructure changes to an inverse dispersion in which the nickel particles are almost discretely distributed in the PSZ matrix. Furthermore, both composition and microstructure of each layer in the sintered ZrO_2–Ni FGM body are quite fine and homogeneous as shown in Figs 3 and 4.

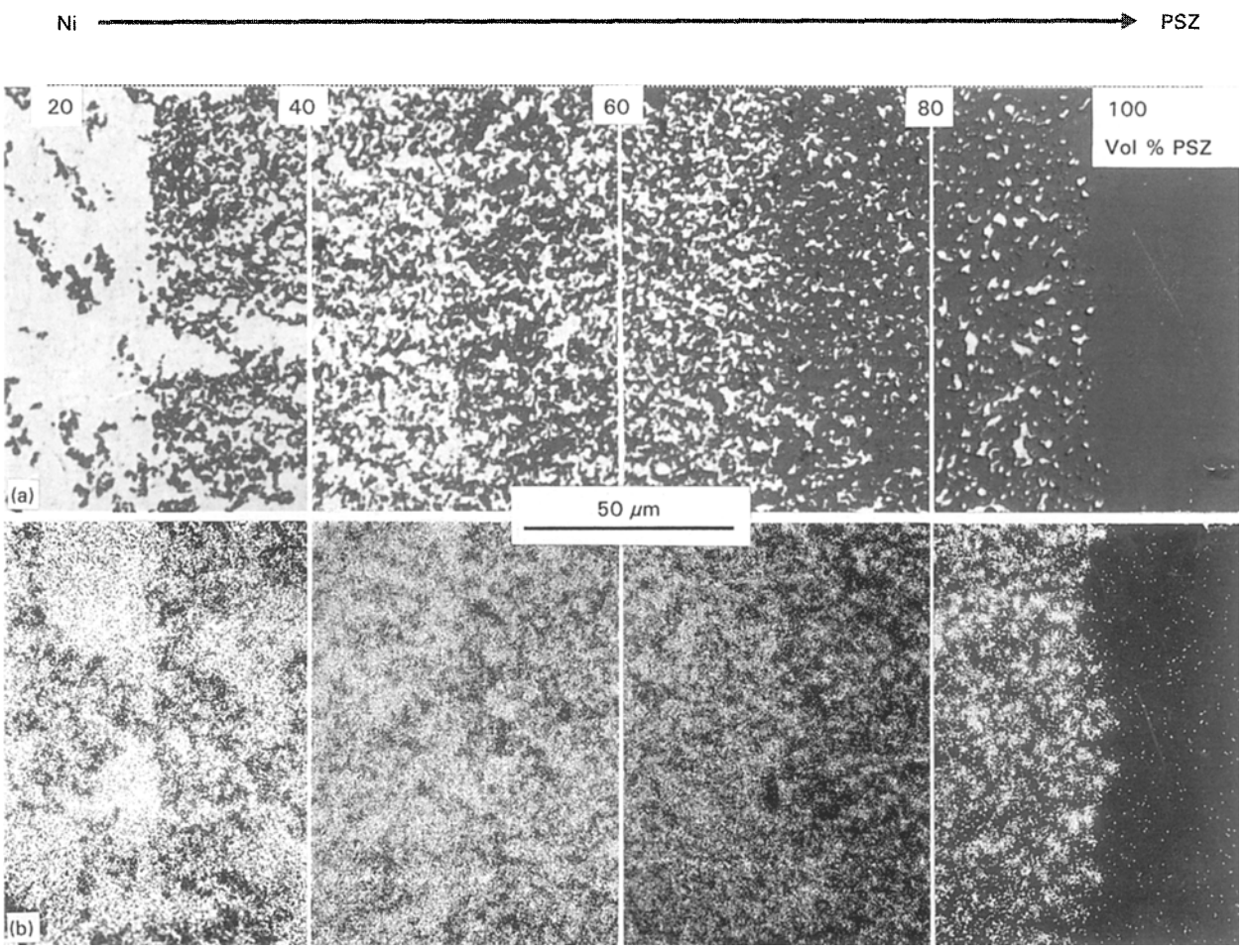

Figure 3 Cross-sectional microstructure of the area with compositional changes in ZrO_2–Ni FGM: (a) optical micrograph and (b) EPMA image of Ni.

3.3. Phase composition and density

The X-ray diffraction patterns of different layers in ZrO_2–Ni FGM indicate that the phase composition consists of nickel, tetragonal zirconia (t-ZrO_2) and a little monoclinic zirconia (m-ZrO_2) as shown in Fig. 5. Clearly there is no reaction between nickel and zirconia in the hot-pressing process, and as the chemical composition varies, the change of phase components is in good agreement with the result of the microstructural observations (Figs 3 and 4).

Figs 3a and 4 reveal that the sintered body of the FGM contains few pores and therefore is almost fully densified. As shown in Fig. 6, the density of ZrO_2–Ni composite increases in a linear way with the increase in Ni vol % due to the higher density of nickel (8.85 $g\,cm^{-3}$) in comparison with the zirconia (5.85 $g\,cm^{-3}$). The composite with 60 vol % Ni contained more pores than the others because of the connective transition of PSZ components according to the fractal analysis [11] and microstructural observation as above (Figs 3 and 4), so its density gradient slightly deviated from linearity. As to the lower value of density at 20 vol % Ni, it was probably related to nickel flowing away in the hot-pressing process, which induced the variation in composition.

3.4. TEM observation

The TEM observation reveals the structure of the ZrO_2–Ni FGM more clearly, as shown in Fig. 7. The interlayers of ZrO_2–Ni FGM comprise nickel, tetragonal and monoclinic zirconia phases which are corroborated by the XRD results (Fig. 7a). In the cooling process after sintering, the PSZ component of the FGM partially transformed from t-ZrO_2 to m-ZrO_2 and exhibits a dual t + m microstructure (Fig. 5a and b). The grains of untransformed t-ZrO_2 are nearly equiaxed and rather uniform in size (Fig. 5c), and they are accompanied by strain fringes due to the difference in thermal expansion coefficient between t-ZrO_2 and the nickel phase (Fig. 7d). The phase interfaces between nickel and zirconia are quite straight and seem to be directly connected (Fig. 7a). Further work must be done to explore the fine structure of Ni/ZrO_2 interfaces as well as the effect of Ni on the t → m transformation in ZrO_2–Ni FGM.

The m-ZrO_2 as well as the nickel has a twinned substructure as shown in Fig. 7b and f. However, the mechanism of the twin's formation in m-ZrO_2 and nickel is not the same. The substructure of m-ZrO_2 is always twinned, which is considered to accommodate the change of shape taking place during the t → m transformation, but the twin in nickel is formed in the hot-pressing process due to its lower stacking fault energy.

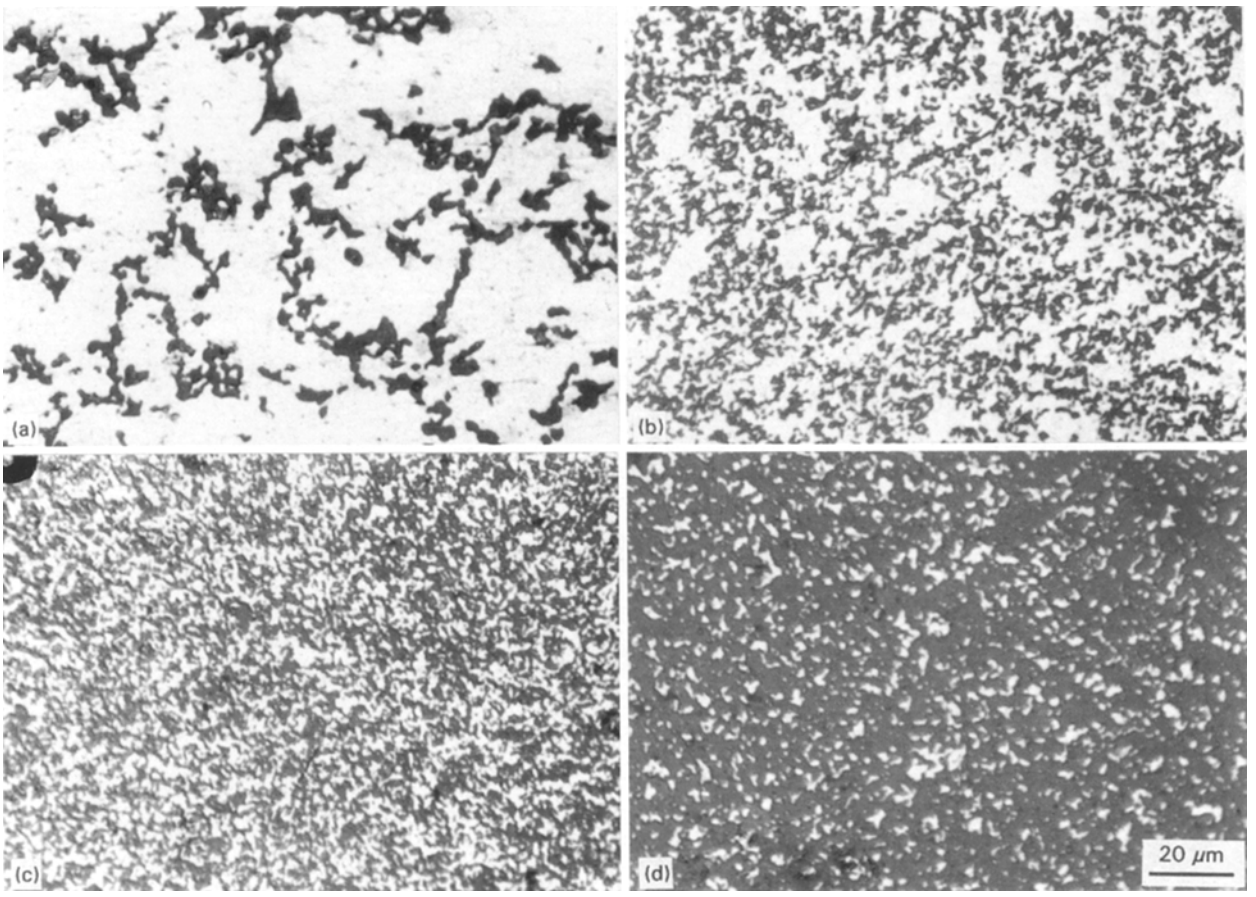

Figure 4 Microstructure of each layer in ZrO_2–Ni FGM: (a) 20, (b) 40, (c) 60 and (d) 80 vol % PSZ.

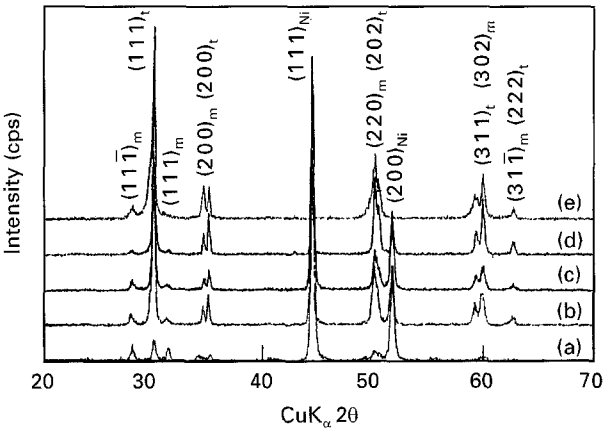

Figure 5 X-ray diffractograms of different layers in ZrO_2–Ni FGM (a) 20, (b) 40, (c) 60, (d) 80, and (e) 100 vol % PSZ.

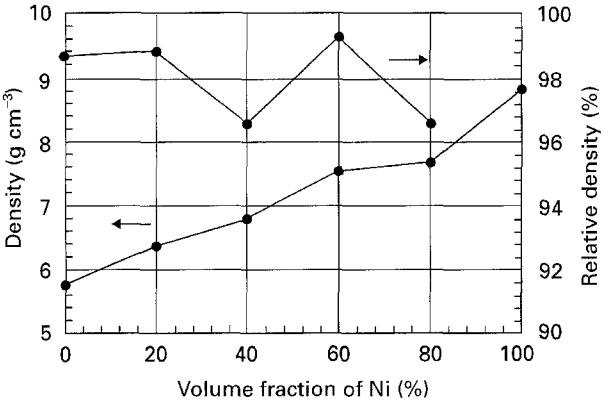

Figure 6 Density and relative density of ZrO_2–Ni composite.

It should be noted that the composition and structure of ZrO_2–Ni FGM are heterogeneous. To be more accurate, they are microscopically inhomogeneous because of the coexistence of several different phases (Figs 5 and 7) and macroscopically inhomogeneous due to the gradient distribution of the chemical composition (Fig. 2). But the conventional composite materials are macroscopically homogeneous in spite of their microscopic heterogeneity. In this sense, a FGM is distinguished from a common composite. On the other hand, the composition and microstructure of ZrO_2–Ni FGM gradually change from one area to another so that they are continuous both in composition and structure (Figs 2 and 3). Thus there is no macroscopic interface in a FGM. This is the difference between ZrO_2–Ni FGM and direct bonding of the two materials ZrO_2/Ni. As a result, ZrO_2–Ni FGM will have the dual advantages of ceramics and metals for practical purposes, and they will be free from fracture of spallation which occurs for metal/ceramic interfaces, giving a reduction in thermal stress. However, it should be indicated that there seems to be a transition in matrix continuity of ZrO_2–Ni FGM at some PSZ/Ni mixing ratio due to the microstructural transition with compositional variation (Figs 3 and 4). This problem would induce a decrease in mechanical properties [9, 11], which could be overcome by suitable control of the FGM's microstructure. For

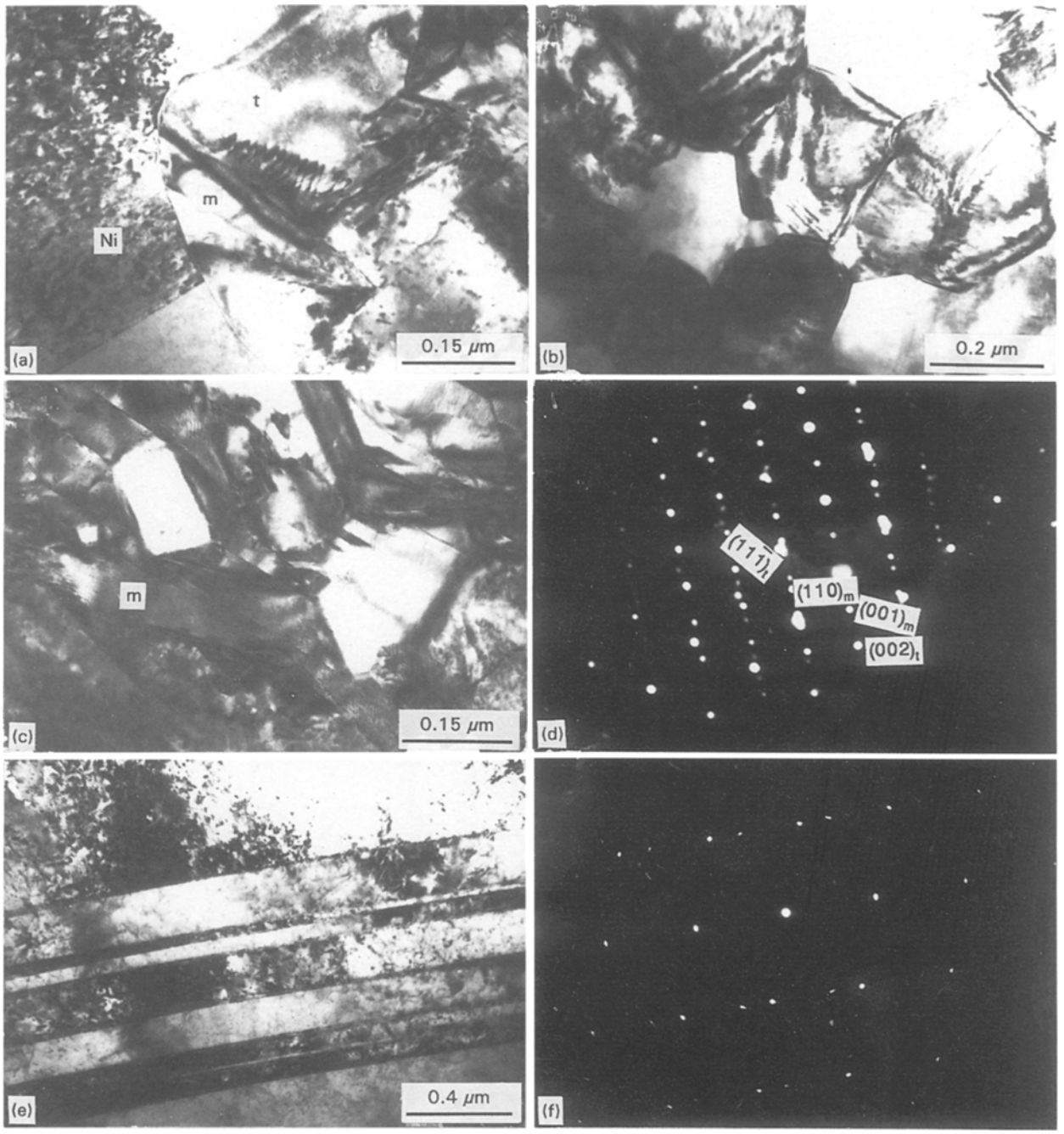

Figure 7 TEM photographs of ZrO_2–Ni FGM showing (a) Ni + t + m mixture, (b) grains and strain fringes in t-ZrO_2, (c) t + m dual phase mixture, (d) their electron diffraction pattern, (e) annealing twins in nickel and (f) their electron diffraction pattern.

example, a metal fibre can be introduced to control the connectivity of the metallic phase in the FGM, and powder metallurgy seems to be the most effective process in this field especially for the high temperature and heavily loaded conditions.

4. Conclusions

1. The dense FGM of ZrO_2–Ni system with stepwise compositional gradation was fabricated by a powder metallurgical process, and possesses the expected distribution gradient in composition and structure.

2. There are no distinct interfaces in the FGM due to the gradient changes of composition and structure. Even on the pre-stacked section where chemical compositions jumped in a stepwise manner both the nickel and zirconia components are continuous in microstructure. Moreover, with the compositional variation, the microstructure of ZrO_2–Ni FGM exhibits a transition from a zirconia particle dispersion in a nickel matrix to an inverse dispersion of nickel in zirconia.

3. The sintered ZrO_2–Ni FGM body consists of nickel, tetragonal and some monoclinic zirconia, and the nickel as well as the monoclinic zirconia phase exhibits a twinned substructure. No reaction product between Ni and ZrO_2 is detected, and the Ni/ZrO_2 phase interfaces may be directly connected. This needs a more in depth investigation.

References

1. M. NIINO, T. HIRAI and R. WATANABE. *J. Jpn. Soc. Compos. Mater.* **13** (1987) 257.
2. A. KAWASAKI and R. WATANABE. *J. Jpn. Inst. Met.* **51** (1987) 525.
3. S. AKAMA. *Jpn. Ceram. Bull.* **24** (1989) 960.
4. K. KOKINI and Y. TAKEUCHI, Proceedings of the 1st International Symposium on FGM, Sendai, Japan, 1990, edited by M. Yamanouchi, M. Koizumi, T. Hiral and I. Shiota, 'Functionally Gradient Materials Forum', Tokyo, Japan p. 31.
5. T. KAWAI, S. MIYAZAKI and M. ARARAGI. *ibid.* p. 191.
6. M. NIINO, A. KUMAKAWA and M. SASAKI. *J. IEE Jpn.* **110** (1990) 35.
7. M. KOIZUMI and K. URABE. *Iron and Steel* **75** (1989) 887.
8. A. KAWASAKI and R. WATANABE. *J. Jpn. Soc. Powder Powder Metall.* **37** (1990) 253.
9. J. C. ZHU, Z. D. YIN and Z. H. LAI, in International Workshop on Frontiers of Advanced Materials, Physics & Technology (IWPM-6), Shenyang, China, 1992; *J. Met. Sci. Technol.* **10** (1994) 188.
10. R. C. GARVIE and M. V. SWAIN. *J. Mater. Sci.* **20** (1985) 1193.
11. K. MURAMATSU, A. KAWASAKI, M. TAYA and R. WATANABE, in Proceedings of the 1st International Symposium on FGM, Sendai, Japan, 1990, edited by M. Yamanouchi, M. Koizumi, T. Hiral and I. Shiota, 'Functionally Gradient Materials Forum', Tokyo, Japan p. 53.

Received 1 February 1994
and accepted 1 December 1995